

## ARTICLES

## Scaling in late stage spinodal decomposition with quenched disorder

Mark F. Gyure,<sup>1,2</sup> Stephen T. Harrington,<sup>1</sup> Richard Strilka,<sup>1</sup> and H. Eugene Stanley<sup>1</sup><sup>1</sup>Center for Polymer Studies, Department of Physics, Boston University, Boston, Massachusetts 02215<sup>2</sup>Hughes Research Laboratories, Malibu, California 90265

(Received 9 March 1995; revised manuscript received 24 July 1995)

We study the late stages of spinodal decomposition in a Ginzburg-Landau mean field model with quenched disorder. Random spatial dependence in the coupling constants is introduced to model the quenched disorder. The effect of the disorder on the scaling of the structure factor and on the domain growth is investigated in both the zero temperature limit and at finite temperature. In particular, we find that at zero temperature the domain size  $R(t)$  scales with the amplitude  $A$  of the quenched disorder as  $R(t) = A^{-\beta} f(t/A^{-\gamma})$  with  $\beta \simeq 1.0$  and  $\gamma \simeq 3.0$  in two dimensions. We show that  $\beta/\gamma = \alpha$ , where  $\alpha$  is the Lifshitz-Slyosov exponent. At finite temperature, this simple scaling is not observed and we suggest that the scaling also depends on temperature and  $A$ . Comparisons of the scaled structure factors for all values of  $A$  at both zero and finite temperature indicate only one universality class for domain growth. We discuss these results in the context of Monte Carlo and cell dynamical models for phase separation in systems with quenched disorder and propose that in a Monte Carlo simulation the concentration of impurities  $c$  is related to  $A$  by  $A \sim c^{1/d}$ .

PACS number(s): 64.60.Ak

## I. INTRODUCTION

Spinodal decomposition has received a great deal of attention in recent years since it is relevant to many materials processing problems and is one of the unsolved problems in statistical mechanics. Much progress has occurred over the past decade in understanding both the early and late time behavior of spinodal decomposition in the simplest systems with no disorder and a single order parameter [1-4], but there is more to learn concerning the important process of spinodal decomposition in disordered systems. Systems with quenched disorder, for example, are interesting because the kinetics of spinodal decomposition differs markedly from the behavior of pure systems. In particular, the usual power law growth of the characteristic domain size  $R \sim t^\alpha$  is thought to change over to a logarithmic growth [5]

$$R \sim (\ln t)^\theta. \quad (1.1)$$

The earliest computational studies of phase separation in systems with quenched disorder were Monte Carlo (MC) simulations performed nearly a decade ago [6-8]. MC simulations are generally inefficient for studying domain growth since diffusion of particles through the system at late stages requires many updates. However, MC simulations have the distinct advantage of introducing the quenched disorder in a very natural way. Using MC simulations, Grest and Srolovitz [6] found evidence of a scaling function relating  $R$  to the concentration of impurities in a two-dimensional Ising model with a non-conserved order parameter, but were unable to confirm the prediction [5] of logarithmically slow domain growth Eq. (1.1). Similar behavior was seen in MC simulations of

a model for simultaneous phase separation and gelation in an Ising-type model with a conserved order parameter [9].

Further progress has recently been made [10,11] using more efficient cell dynamical methods [12]. These cell dynamical simulations were able to probe the late stage behavior for cases of both conserved and nonconserved order parameter by introducing the disorder as a phenomenological parameter in the Ginzburg-Landau free energy [13]. Using cell dynamical methods, Puri *et al.* [10,11] were able to observe the logarithmically slow domain growth [5] for both conserved and nonconserved order parameter, although the exponent  $\theta$  in the predicted behavior Eq. (1.1) for the case of a conserved order parameter appeared to vary with the amplitude of the quenched disorder. This could be due in part to the systems not having reached their asymptotic behavior; even using the cell dynamical approach, simulation of disordered systems is computationally demanding due to the logarithmically slow growth.

Here we study a time-dependent Ginzburg-Landau (TDGL) model and consider scaling of the domain size as a function of the quenched disorder both in the zero temperature limit and for  $T > 0$ . For  $T = 0$ , we expect that domain growth will effectively stop as various parts of the system fall into metastable states from which they cannot escape. Although the  $T = 0$  limit is clearly unphysical, domain growth pinning is seen in experimental systems with quenched disorder [14]. Studying the TDGL model in this limit gives us the opportunity to study the effect of a single parameter, the quenched disorder  $A$ , on the dynamics of domain growth. We find scaling that relates the characteristic domain size  $R$  to the phenomenological parameter  $A$  that describes the disorder in the model.

We also examine the behavior of this model at finite temperature. We find that this simple scaling does not hold and propose a form for the exponent  $\theta$  in Eq. (1.1).

The rest of this paper is organized as follows. In Sec. II, we describe the time-dependent Ginzburg-Landau model with quenched disorder and briefly discuss its numerical implementation. In Sec. III we describe the results of our simulations and propose a scaling form that is consistent with these results. Finally, in Sec. IV we place these results in context with results for the Monte Carlo and cell dynamical models described above.

## II. THE MODEL AND ITS SCALING PROPERTIES

In this section we briefly review the time-dependent Ginzburg-Landau equation and the rescaling of the variables that leads to the Cahn-Hilliard equation [15], the basis of our simulation model. In addition, we introduce quenched disorder into the Cahn-Hilliard equation [10,11] via additional random, static coupling constants taken from a uniform distribution of width  $A$ . We present a scaling hypothesis for the model based on observations made in previous work [10,11].

Consider a system with two independent species. The order parameter  $\phi$  is defined [1] to be the difference in the local concentration of these two species

$$\phi \equiv c_1 - c_2. \quad (2.1)$$

For a conserved order parameter, the local concentration difference obeys a continuity equation of the form

$$\frac{\partial}{\partial t} \phi(\mathbf{r}, t) = -\nabla \cdot \mathbf{j}(\mathbf{r}, t) + \zeta(\mathbf{r}, t). \quad (2.2)$$

Here the current is

$$\mathbf{j}(\mathbf{r}, t) = -M \nabla \mu(\mathbf{r}), \quad (2.3)$$

where  $M$  is the mobility (assumed to be constant),  $\mu(\mathbf{r})$  is the chemical potential (the variational derivative of the free energy), and  $\zeta(\mathbf{r}, t)$  is Gaussian-distributed random noise that satisfies

$$\langle \zeta(\mathbf{r}, t), \zeta(\mathbf{r}', t') \rangle = -2k_B T M \nabla^2 \delta(\mathbf{r} - \mathbf{r}') \delta(t - t'), \quad (2.4)$$

where the angular brackets represent a thermal average over many different configurations. This term guarantees that the proper equilibrium state is achieved. In the TDGL model one usually chooses the Ginzburg-Landau free energy functional [1]

$$F = \int d\mathbf{r} \left\{ \frac{1}{2} \kappa |\nabla \phi|^2 - \frac{1}{2} \rho \phi^2 + \frac{1}{4} u \phi^4 \right\}. \quad (2.5)$$

Combining the continuity equation Eq. (2.2) with the free energy Eq. (2.5) yields

$$\frac{\partial \phi}{\partial t} = M \nabla^2 \{ -\kappa \nabla^2 \phi - \rho \phi + u \phi^3 \} + \zeta. \quad (2.6)$$

The continuity equation Eq. (2.2) guarantees conserva-

tion of the order parameter  $\phi$ ; this is known as model B. Model B is a time-dependent Ginzburg-Landau model or relaxation model since the time evolution of the order parameter depends only on the minimization of the free energy functional Eq. (2.5).

The order parameter  $\phi$  is redefined by scaling the phenomenological parameters  $M$ ,  $\kappa$ ,  $\rho$ , and  $u$  in Eq. (2.6) as well as the dynamical variables  $\mathbf{r}$  and  $t$  to obtain a simplified equation of motion for the rescaled order parameter. This is known as the Cahn-Hilliard equation [15] and has the form

$$\frac{\partial}{\partial \tau} \psi = \frac{1}{2} \nabla^2 (-\psi + \psi^3 - \nabla^2 \psi) + \sqrt{\epsilon} \xi. \quad (2.7)$$

The transformation that rescales model B into the Cahn-Hilliard model, following Grant *et al.* [16] and Rogers *et al.* [17], is

$$\mathbf{x} \equiv \left( \frac{\rho}{\kappa} \right)^{1/2} \mathbf{r}, \quad (2.8a)$$

$$\tau \equiv \frac{2M\rho^2}{\kappa} t, \quad (2.8b)$$

$$\psi \equiv \left( \frac{u}{\rho} \right)^{1/2} \phi, \quad (2.8c)$$

$$\epsilon \equiv \frac{k_B T u}{\rho^2} \left( \frac{\rho}{\kappa} \right)^{d/2}. \quad (2.8d)$$

Hence, from Eq. (2.4),

$$\begin{aligned} & \langle \xi(\mathbf{x}, \tau), \xi(\mathbf{x}', \tau') \rangle \\ &= -2k_B T u / \rho^2 \left( \frac{\rho}{\kappa} \right)^{1/2} M \nabla^2 \delta(\mathbf{x} - \mathbf{x}') \delta(\tau - \tau'). \end{aligned} \quad (2.9)$$

The formulation of model B in these variables clearly shows that this model involves only a single parameter  $\epsilon$  proportional to the temperature.

To incorporate quenched disorder into model B, it is conventional to introduce a spatial dependence in the parameters  $\rho$  and  $u$  of Eq. (2.5) [13]. Consider couplings of the form  $\rho = \rho_0 + \delta\rho(\mathbf{x})$  and  $u = u_0 + \delta u(\mathbf{x})$ , where  $\rho_0$  and  $u_0$  are identified with the free energy in the absence of disorder. After performing the transformation of variables leading to Eq. (2.7), the time-dependent Ginzburg-Landau equation with quenched disorder becomes

$$\begin{aligned} \frac{\partial}{\partial t} \psi = & -\frac{1}{2} \nabla^2 \left[ \left( 1 + \frac{\delta\rho(\mathbf{x})}{\rho_0} \right) \psi \right. \\ & \left. - \left( 1 + \frac{\delta u(\mathbf{x})}{u_0} \right) \psi^3 + \nabla^2 \psi \right] + \sqrt{\epsilon} \xi. \end{aligned} \quad (2.10)$$

We choose for simplicity the factors [13]

$$\frac{\delta\rho(\mathbf{x})}{\rho_0} \quad \frac{\delta u(\mathbf{x})}{u_0} \quad (2.11)$$

to be random variables taken from a uniform distribution of width  $A$ , thereby giving a random spatial dependence to the rescaled couplings in the model.

Equation (2.10) is a generalization of the Cahn-Hilliard equation Eq. (2.7). Earlier results clearly indicate that the crossover time  $t_x$  from the early stage algebraic growth to logarithmically slow growth at later times increases as the amplitude  $A$  of the quenched disorder decreases [11]. Thus it is appropriate to consider two distinct time domains separated by a crossover region characterized by a time  $t_x$ . For  $t \ll t_x$  we expect the domain size to grow as

$$R(t) \sim t^\alpha, \quad (2.12)$$

where  $\alpha = 1/3$  from the Lifshitz-Slyosov theory [18]. This exponent has been observed in a wide variety of TDGL and cell dynamical simulations [3,4] with a conserved order parameter. For  $t \gg t_x$  we expect that the domain size at any time in the slower growth region will scale as  $R(t) \sim A^{-\beta}$ . Finally, the observation by Puri and Parekh [11] that the crossover time  $t_x$  increases for decreasing disorder amplitude suggests that

$$t_x \sim A^{-\gamma} \quad (2.13)$$

and hence the scaling form

$$R(t) \sim A^{-\beta} f(t/t_x) \sim A^{-\beta} f(tA^\gamma). \quad (2.14)$$

From (2.12) and (2.14) it follows that

$$\beta = \alpha\gamma. \quad (2.15)$$

### III. CALCULATIONS AND RESULTS

We now describe the results of our computer simulations that verify the scaling hypothesis (2.14). First we calculate the average domain size  $R(t)$  of the system. Since there is only *one* relevant length scale in a sys-

TABLE I. Asymptotic values  $R_f$  of the domain size for various values of the quenched disorder as calculated from the simulations for both  $T = 0$  and  $T > 0$ . We used a  $256 \times 256$  lattice with spacing  $\Delta x = 0.30$ . The evolution of Eq. (2.9) was performed for  $3 \times 10^6$  updates with a time interval of 0.15.

Amplitude	$T = 0$		$T > 0$	
	Runs	$R_f$	Runs	$R_f$
0.25	23	$6.2 \pm 0.1$		
0.30	26	$5.26 \pm 0.07$	7	$7.4 \pm 0.1$
0.35	15	$4.45 \pm 0.05$	10	$6.4 \pm 0.1$
0.40	18	$3.92 \pm 0.04$	8	$5.3 \pm 0.2$
0.45	18	$3.50 \pm 0.03$	6	$4.6 \pm 0.1$

tem undergoing spinodal decomposition [1], any characteristic length  $R$  is proportional to the domain size. We choose  $R$  to be the inverse of the first moment  $k_1$  of the spherically averaged structure factor  $S(k, t)$ , which is the structure factor  $S(\mathbf{k}, t) \equiv \langle \int d\mathbf{r} e^{-i\mathbf{k} \cdot (\mathbf{r} - \mathbf{r}')} g(\mathbf{r} - \mathbf{r}') \rangle$  averaged over the two-dimensional density of states. As usual,  $S(\mathbf{k}, t)$  is the Fourier transform of the density-density correlation function  $g(\mathbf{r} - \mathbf{r}')$ . The angular brackets represent the averaging over many realizations of the disorder parametrized by  $A$  (see Table I). Since we are considering systems with a conserved order parameter, the domain size scales as  $R(t) \sim 1/k_{\max}$ , where  $k_{\max}$  is the value at which  $S(\mathbf{k}, t)$  is maximum. In our simulations, however, we use the first moment  $k_1$  of  $S(k, t)$  (which is equivalent [1]), since the peak maximum is difficult to determine accurately.

We integrate the equation of motion Eq. (2.10) directly, using the central difference approximation for the spatial derivatives. Following Rogers *et al.* [17], we use a time step of  $\Delta t = 0.15$  and lattice spacing  $\Delta x = 0.30$  to ensure the stability of Eq. (2.10). We allow for  $3 \times 10^6$  updates for each run on a two-dimensional lattice of size  $256 \times 256$  and calculate  $S(\mathbf{k}, t)$  at logarithmically spaced time intervals. We obtain the results discussed in this section by averaging over 15–25 realizations of  $A$  (see Table I),

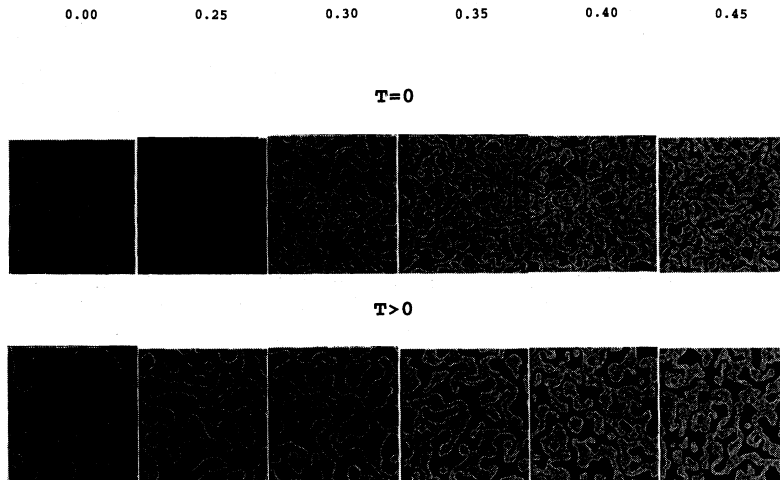


FIG. 1. Typical simulation results showing the domains for various values of  $A$  after  $3 \times 10^6$  updates. The top row is the case  $T = 0$  and the bottom row is  $T > 0$ . Note the decreasing domain size as  $A$  increases. Also, the interface between the two phases is thicker and rougher for  $T > 0$  compared to  $T = 0$ .

ranging from 0.0 to 0.45.

We start with a homogeneous two-dimensional system with the rescaled order parameter  $\psi$  initialized from a uniform random distribution in the range  $-0.005$  to  $0.005$ . For  $T > 0$ , we use a noise amplitude  $\sqrt{\epsilon} = 0.5$ , see Eq. (2.10). In Fig. 1 we display the value of  $\psi$  for every choice of  $A$ . Each snapshot is made after  $3 \times 10^6$  updates in the time evolution. As can be seen from these snapshots, the larger the disorder parameter  $A$ , the smaller the asymptotic domain size. The domains gradually decrease in size as we increase  $A$ . This holds for simulations at both  $T = 0$ , the top row, and  $T > 0$ , the bottom row. Note that the domains have rougher and wider interfaces for  $T > 0$ .

Following the discussion in Sec. II, we calculate the domain size  $R(t)$  from the first moment of the spherically averaged structure factor. In Fig. 2(a) we display our results for  $S(k, t)$  vs wave number  $k \equiv |\mathbf{k}|$ , averaged over 20 runs with no quenched disorder. As expected

[1,17],  $S(k, t)$  displays a peak that increases with time to smaller values of wave number  $k$ . The peak of the structure factor is larger and occurs at a greater value of  $k$  compared to the case with quenched disorder [see Fig. 2(b)]. In fact, the finite value of the asymptotic domain size for  $A = 0$  only exists due to the finite size of the lattice. This behavior is contrasted with Fig. 2(b), which shows  $S(k, t)$  for  $A = 0.45$ . As Fig. 2(b) suggests, the peak of  $S(k, t)$  reaches a maximum value at  $k > 2\pi/L$ .

Figure 3 shows the domain size  $R(t)$  at (a)  $T = 0$  and (b)  $T > 0$  for each value of  $A$ . As can be seen in Fig. 3(a),  $R(t)$  becomes constant after  $10^5 - 10^6$  updates. For  $A = 0.45$ ,  $R(t)$  is constant after  $2 \times 10^5$  updates, while the domain size for  $A = 0.25$  is not constant even after  $3 \times 10^6$  updates. However, we expect that for even small values of  $A$ ,  $R(t)$  becomes constant. This behavior of  $R(t)$  is called *pinning* and is a hallmark of quenched disorder. As we increase the amplitude of the quenched disorder (increase the concentration of impurities), the

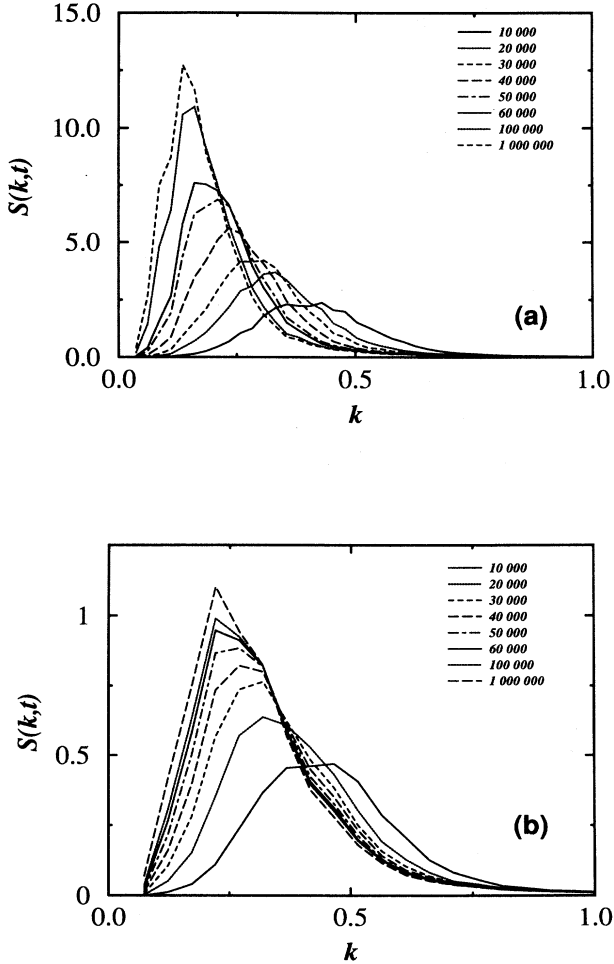


FIG. 2. (a) Spherically averaged structure factor  $S(k, t)$  vs wave number  $k$  for  $A = 0$  at various times. The peak value increases with time and approaches  $k = 0$ . (b)  $S(k, t)$  vs  $k$  for  $A = 0.45$ . Note that  $S(k, t)$  is smaller and  $k_{\max}$  is larger than in (a).

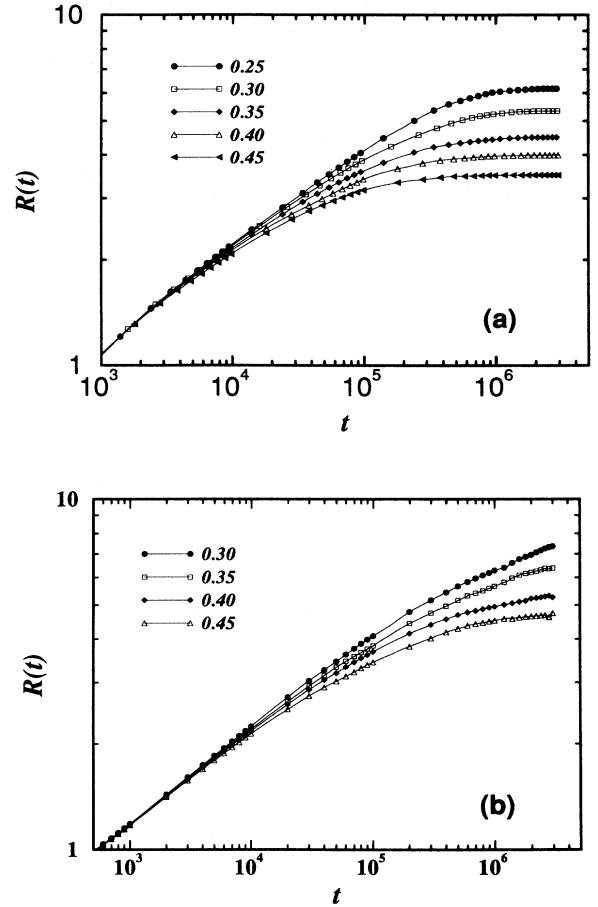


FIG. 3. (a) Double logarithmic plot of the average domain size  $R(t)$  vs time  $t$  at  $T = 0$  for several values of  $A$ . The pinning regime is clearly reached for all disorder amplitudes except, possibly, for  $A = 0.25$ . The  $t^{1/3}$  behavior is apparent at short times, while  $R \sim A^{-1}$  is found in the late stages. (b)  $R(t)$  vs  $t$  for  $T > 0$  for several values of  $A$ . Note that pinning is not observed for any  $A$ .

domain growth stops and eventually becomes pinned. As Fig. 3(b) shows, in the case of  $T > 0$  the domains become larger for each value of  $A$ , but no pinning behavior is observed. In fact, the domains continue to grow throughout the duration of the simulation, as expected from [5]. In both cases, two distinct time regimes are found: a rapid growth in the domain size during the first  $10^3 - 10^4$  updates, followed by a slower growth after some crossover region, characterized by a time  $t_x$ , that is dependent on the amplitude of the quenched disorder.

Since the scaling hypothesis Eq. (2.14) was obtained from considering the late stage growth behavior where  $t \gg t_x$ , we are interested in the scaling behavior of the asymptotic domain size. Figure 4 shows the asymptotic values  $R_f$  for each value of  $A$  for (a)  $T = 0$  and (b)  $T > 0$ . We find a linear relation, confirming the first part of the scaling hypothesis, namely, that the domain size at late times scales as  $R \sim A^{-\beta}$  with  $\beta \simeq 1$ . We also consider scaling of the crossover time  $t_x$  for each  $A$ . We assume that the crossover time scales as  $t_x \sim A^{-\gamma}$ , where  $\gamma \simeq 3$  from Eq. (2.15). Figure 5 shows the simulation results for  $R(t)$  rescaled by Eq. (2.14) with  $\beta = 1, \gamma = 3$ .

Notice that the zero temperature result, shown in Fig. 5(a), collapses quite well over four decades in rescaled time, clearly confirming the scaling hypothesis. The finite temperature result [Fig. 5(b)] scales well over the early time region only, with a clear breakdown in scaling at late times. This suggests that the exponent  $\theta$  in Eq. (1.1) has a functional dependence on the amplitude

of the quenched disorder and the temperature

$$\theta = \theta(A, T). \quad (3.1)$$

We discuss reasons for this in Sec. IV.

We now turn to the question of universality of the domain growth in the presence of quenched disorder at both zero and finite temperature. Previous Monte Carlo simulations of the two-dimensional Ising model with random ferromagnetic bonds [19] show both pure and random systems to be in the same universality class for domain growth with a nonconserved order parameter. In Fig. 6 we show a plot of the scaled structure factor  $S(k, t)[k_1(t)]^2$  versus  $k(t)/k_1(t)$  for different values of the disorder  $A$  at zero temperature and two different times. The collapse of the simulation data indicates that the scaling of the structure factor is independent of  $A$ . In Fig. 7 we show the scaled structure factor for the finite temperature results also at two different times. For this case, we again see that the scaled  $S(k, t)$  is independent of  $A$ , as demonstrated by Puri and Parekh [11] with their cell dynamical model. Finally, in Fig. 8 we show

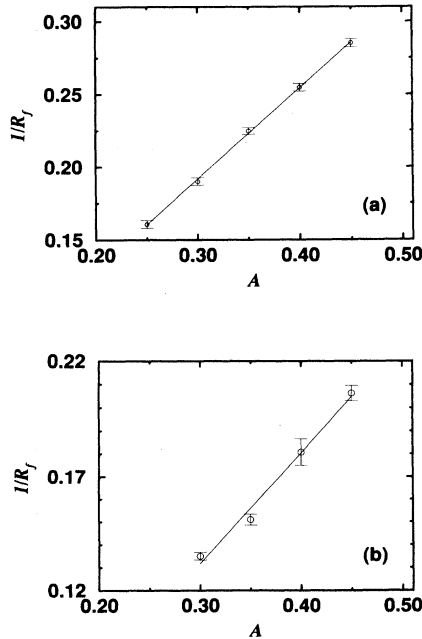


FIG. 4. (a) Inverse of the asymptotic domain size  $1/R_f$  vs disorder amplitude  $A$  for  $T = 0$ .  $R_f$  is taken to be the average domain size after  $3 \times 10^6$  updates. The linear relation confirms the scaling hypothesis Eq. (2.13) with  $\beta = 1$ . (b)  $1/R_f$  vs  $A$  for  $T > 0$ . Note the deviations from a linear relation.

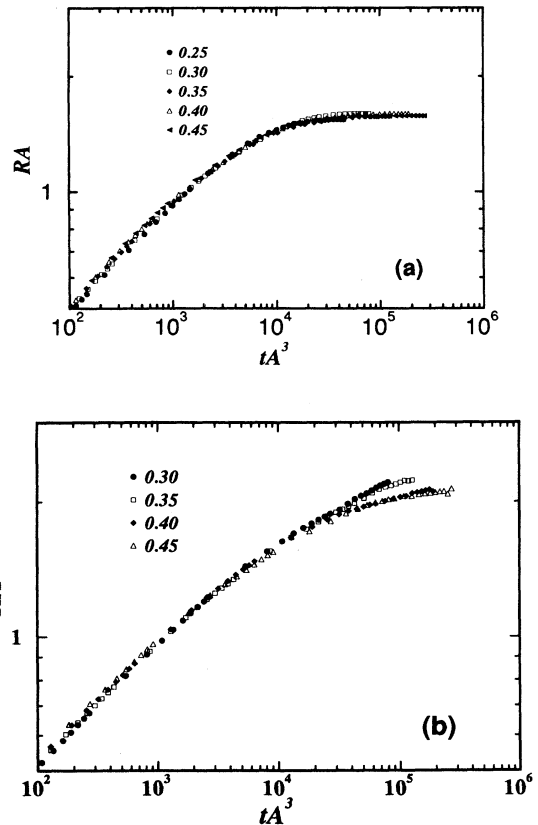


FIG. 5. (a) Scaled domain size  $RA$  vs scaled time  $tA^3$  for  $T = 0$ , using  $\beta = 1$  and  $\gamma = 3$  in the scaling relation Eq. (2.13). The collapse onto a single curve further confirms our scaling hypothesis. (b) Same plot as (a) using simulations with  $T > 0$ .

the scaled structure factor for different values of  $A$  and  $T$ . The data collapse indicates that the scaling of the structure factor is independent of both disorder amplitude and temperature and supports the results of Bray and Humayun [19] for the random bond Ising model with a nonconserved order parameter.

#### IV. DISCUSSION

We find that a time-dependent Ginzburg-Landau model with quenched disorder is capable of reproducing similar results to those found in earlier Monte Carlo simulations [6–8], more recent cell dynamical simulations [10–12], and other TDGL simulations [20]. Our main interest here is the determination of the scaling function relating the domain size  $R$  to the amplitude of the disorder  $A$ . For  $T = 0$ , we find scaling similar to that proposed by

Grest and Srolovitz [6] as well as Glotzer *et al.* [9] in MC simulations. Grest and Srolovitz found  $\alpha = 1/2$  while Glotzer *et al.* found  $\alpha = 1/4$  rather than the  $1/3$  observed in our TDGL simulations. The reason for the different values of  $\alpha$  is that MC simulations rarely yield the predicted Lifshitz-Slyozov growth exponent of  $1/3$  since particle diffusion in a MC simulation takes many more updates than in a TDGL simulation. We expect that at low temperatures a MC simulation using an accelerated algorithm [21] or simply allowed to run sufficiently long will find a similar scaling function with  $\alpha = 1/3$ .

Nevertheless, a comparison of the scaling functions for the zero temperature models described above enables us to find a relationship between the phenomenological disorder parameter  $A$  and the concentration  $c$  of quenched impurities used in Monte Carlo simulations. The scaling form suggested by MC simulations is  $R = c^{-\beta'} f(tc^{\gamma'})$

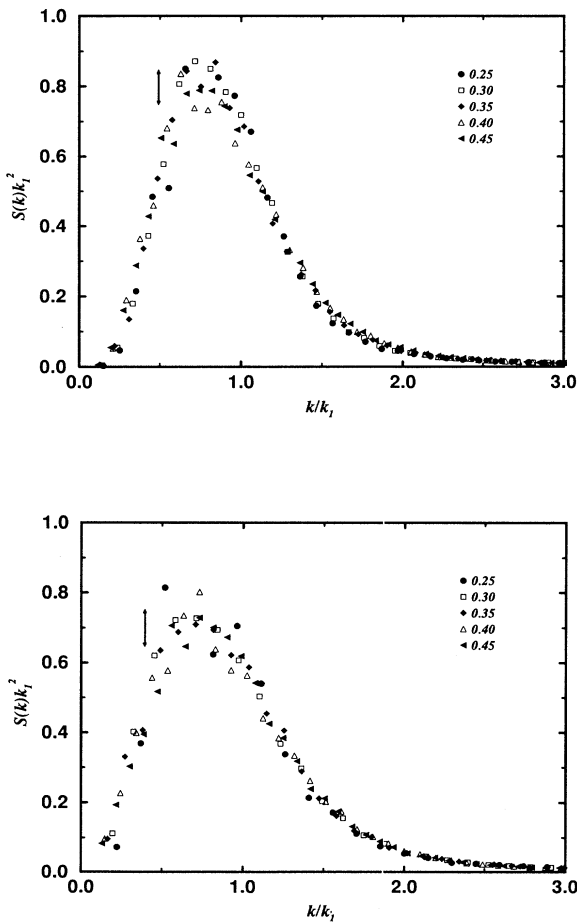


FIG. 6. (a)  $S(k, t)[k_1(t)]^2$  versus  $k(t)/k_1(t)$  for different values of the disorder  $A$  at zero temperature after  $10^5$  updates. The typical statistical error around the peak value is indicated by the arrow, while the statistical error around the tails is comparable to the symbol size. (b) After  $10^6$  updates.

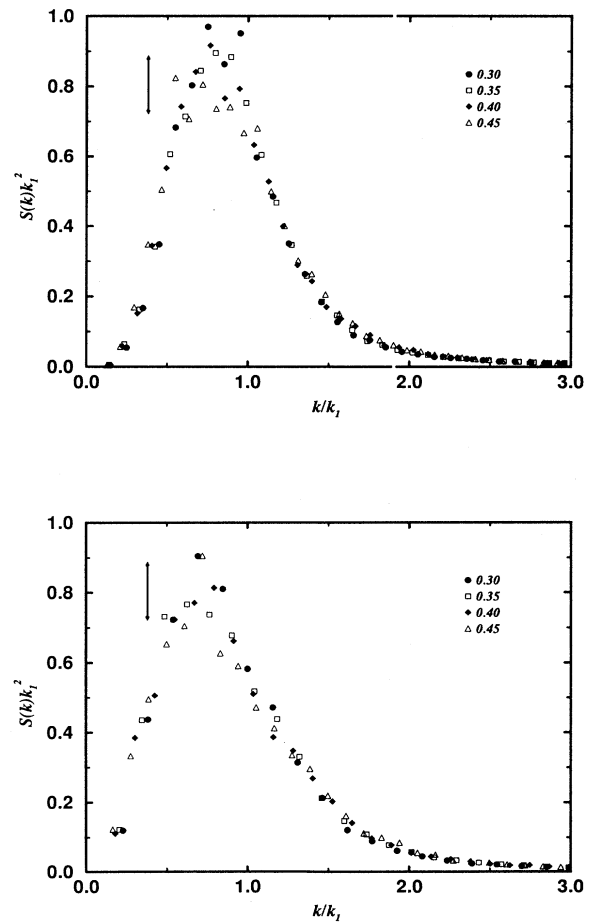


FIG. 7. (a)  $S(k, t)[k_1(t)]^2$  versus  $k(t)/k_1(t)$  for different values of the disorder  $A$  at finite temperature after  $10^5$  updates. The arrow represents the typical statistical error around the peak value. (b) After  $10^6$  updates.

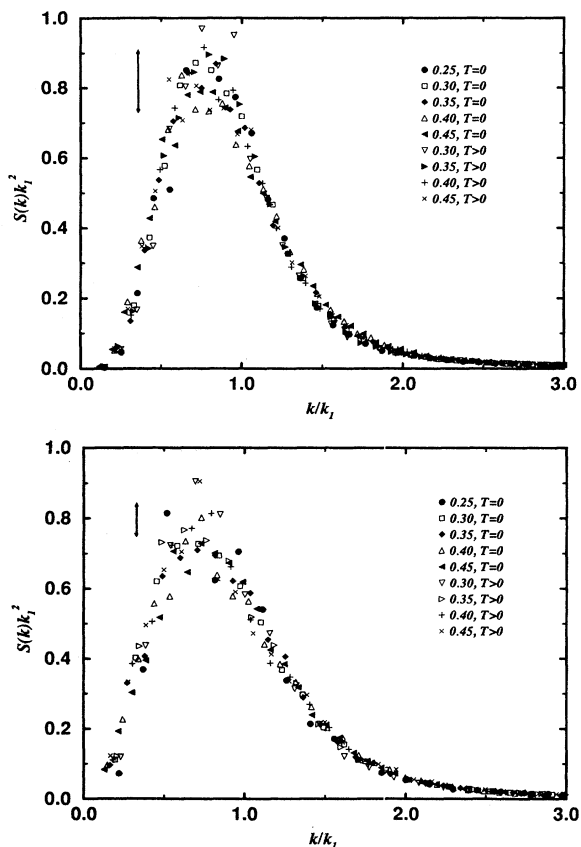


FIG. 8. (a) Rescaled  $S(k, t)$  for both  $T = 0$  and  $T > 0$  for all values of  $A$  after  $10^5$  updates. Note that both the  $T = 0$  and the  $T > 0$  structure factors have the same scaling behavior. (b) After  $10^6$  updates.

with  $\beta' = 1/d$  [9]. The scaling form suggested by our simulations is given by Eq. (2.14) as  $R = A^{-\beta} f(tA^\gamma)$  with  $\beta \simeq 1$ . Since we expect the domain size to scale the same way in both models, we anticipate the relationship

$$A \sim c^{1/d} \quad (4.1)$$

between the amplitude of the quenched disorder and the

impurity concentration. This result indicates that direct MC simulations can be replaced by TDGL simulations or even more efficient cell dynamical simulations, since the relationship between the amplitude of the quenched disorder can now be understood directly in terms of the impurity concentration for a given model.

We note that the scaling found in the simulations discussed above was observed either at zero temperature [6] or effectively at zero temperature [9]. As our results in Fig. 5(b) show, the scaling behavior for quenched disorder models at finite temperature is more complicated. Puri and Parekh [11] observed that the asymptotic behavior of their cell dynamical model was not independent of the disorder parameter  $A$ . Similarly, the MC results of Grest and Srolovitz at  $T > 0$  also suggest that the asymptotic behavior depends on the concentration of impurities. Thus we do not expect that the simple scaling hypothesis Eq. (2.14) would be valid for  $T > 0$ . For late stage domain growth, we expect that the exponent  $\theta$ , in Eq. (1.1), is a function of  $A$  and  $T$ . However, a scaling function describing both the finite and zero temperature behavior of quenched disorder models might still exist. A detailed study of one or more of these models (MC, TDGL, or cell dynamical) spanning a range of temperature and disorder parameters would likely shed considerable light on this matter. Such a study would involve a large computational effort and is well beyond the scope of the present work.

Finally, we suggest that the type of scaling behavior found in a variety of quenched disorder models should be experimentally observable. Indeed, experiments could test the validity of the TDGL model discussed here and could provide interesting insights into the universality of the scaling we report.

#### ACKNOWLEDGMENTS

We thank L. A. N. Amaral, A. Coniglio, R. Cuerno, S. C. Glotzer, S. Havlin, and S. Sastry for helpful discussions. The Center for Polymer Studies is supported in part by funds from the NSF. S.T.H. thanks the NIH for financial support. All simulations were done using the 32-node CM-5 at Boston University's Center for Computational Science.

- [1] J.D. Gunton, M. San Miguel, and P.S. Sahni, in *Phase Transitions and Critical Phenomena*, edited by C. Domb and J.L. Lebowitz (Academic, London, 1983), Vol. 8.
- [2] J.G. Amar, F.E. Sullivan, and R.D. Mountain, *Phys. Rev. B* **37**, 196 (1988); T.M. Rogers and R.C. Desai, *ibid.* **39**, 11956 (1989); C. Roland and M. Grant, *Phys. Rev. Lett.* **60**, 2657 (1988); *Phys. Rev. B* **39**, 1197 (1989).
- [3] T.M. Rogers, K.R. Elder, and R.C. Desai, *Phys. Rev. B* **37**, 9638 (1988); R. Toral, A. Chakrabarti, and J.D. Gunton, *Phys. Rev. Lett.* **60**, 2311 (1988); *Phys. Rev. B* **39**, 4386 (1989); *Phys. Rev. E* **47**, 3025 (1993);

A. Coniglio, and M. Zannetti, *Europhys. Lett.* **10**, 575 (1989).

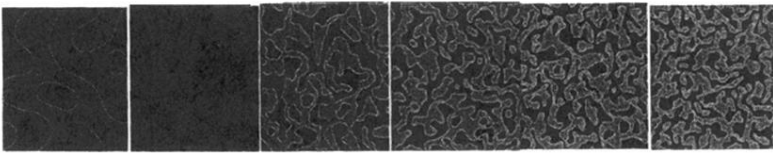
- [4] Y. Oono and S. Puri, *Phys. Rev. Lett.* **58**, 836 (1987); *Phys. Rev. A* **38**, 434 (1988); S. Puri, *Phys. Lett.* **134A**, 205 (1988); S. Puri and Y. Oono, *J. Phys. A* **21**, L755 (1988); *Phys. Rev. A* **38**, 1542 (1988); H. Furukawa, *Phys. Rev. B* **40**, 2341 (1989).
- [5] D. Huse and C. Henley, *Phys. Rev. Lett.* **54**, 2708 (1985).
- [6] G. Grest and D.J. Srolovitz, *Phys. Rev. B* **32**, 3014 (1985).
- [7] D.J. Srolovitz and G. Grest, *Phys. Rev. B* **32**, 3021

- (1985).
- [8] D.J. Srolovitz and G.N. Hassold, *Phys. Rev. B* **35**, 6902 (1987).
- [9] S. Glotzer, M.F. Gyure, F. Sciortino, A. Coniglio, and H.E. Stanley, *Phys. Rev. Lett.* **70**, 3275 (1993); *Phys. Rev. E* **49**, 247 (1994).
- [10] S. Puri, D. Chowdhury, and N. Parekh, *J. Phys. A* **24**, L1087 (1991).
- [11] S. Puri and N. Parekh, *J. Phys. A* **25**, 4127 (1992).
- [12] Y. Oono and S. Puri, *Phys. Rev. Lett.* **58**, 836 (1987).
- [13] In MC simulations, the concentration of quenched impurities is directly proportional to the number of inactive or blocked sites on the lattice; in cell dynamical simulations, the disorder is introduced by modifying the phenomenological constants, see, e.g., S.K. Ma, *Modern Theory of Critical Phenomena* (Benjamin, Reading, MA, 1976).
- [14] R. Bansil, J. Lal, and B.L. Carvalho, *Polymer* **33**, 2961 (1992).
- [15] J.W. Cahn and J.E. Hilliard, *J. Chem. Phys.* **28**, 258 (1958).
- [16] M. Grant, M. San Miguel, J. Vinals, and J.D. Gunton, *Phys. Rev. B* **31**, 3027 (1985).
- [17] T.M. Rogers, K.R. Elder, and R.C. Desai, *Phys. Rev. B* **37**, 9638 (1988).
- [18] I.M. Lifshitz and V.V. Slyosov, *J. Phys. Chem. Solids* **19**, 35 (1961).
- [19] A.J. Bray and K. Humayun, *J. Phys. A* **24**, L1185 (1991).
- [20] F. Sciortino, R. Bansil, P. Alstrøm, and H.E. Stanley, *Phys. Rev. E* **47**, 4615 (1993).
- [21] G.T. Barkema, J.F. Marko, and J. de Boer, *Europhys. Lett.* **26**, 653 (1994).



0.00      0.25      0.30      0.35      0.40      0.45

$T=0$



$T>0$

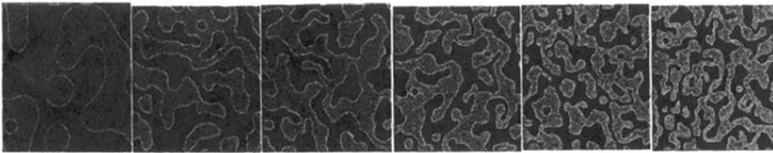


FIG. 1. Typical simulation results showing the domains for various values of  $A$  after  $3 \times 10^6$  updates. The top row is the case  $T = 0$  and the bottom row is  $T > 0$ . Note the decreasing domain size as  $A$  increases. Also, the interface between the two phases is thicker and rougher for  $T > 0$  compared to  $T = 0$ .